brachytherapy as monotherapy for clinical T1/T2 carcinoma of the prostate gland at our institution. One patient did not return for followup radiographs, leaving 158 patients for analysis. Table 1 details the characteristics of all 158 patients. No patient received supplemental external beam radiotherapy. All 158 patients received I-125 seeds as free seeds. A total of 11,240 seeds were used. The radioactive source strength varied from 0.31 to 0.38 mCi per seed.

About 1 month before the procedure, a transrectal ultrasound (TRUS) volume study was undertaken in all patients. Seed placement was preplanned. TG 43 formalism was used in the planning (8). The planning target volume included the prostate gland, with 3 to 5 mm margins in all directions except the posterior one, and treatment planning used a peripheral or a modified peripheral approach. The prescribed dose was 145 Gy. VariSeed 7.1 (Varian Medical Systems, Palo Alto, CA) was used both in calculating the preoperative prostate volume and in planning seed placement. Extraprostatic seed placement was not planned.

Implants were performed with standard techniques. When unexpected pubic arch interference (PAI) occurred during implantation and parallel needle insertion was impossible, the patient was repositioned into an extended lithotomy position to increase pelvic rotation so that PAI was reduced. When this problem was solved by the manipulation, and when parallel needle insertion was possible from the planned hole of the template, it was judged that PAI was absent. When this problem was not solved by the manipulation, and oblique needle insertion was undertaken through a more inferior or medial hole of the template than that planned, it was judged that PAI was present.

Three months after the implantation procedure, all patients underwent a series of radiographs (orthogonal chest radiographs, a kidney–ureter–bladder [KUB] radiograph, and a posteroanterior pelvic radiograph) to document seed migration and sites of migration. All radiographs were reviewed by a single radiologist (A.S.). Seeds were scored as migrated when they were visualized radiographically outside the true anatomic location. Seeds misplaced to periprostatic tissues or seminal vesicles were not scored as migrated.

The following information was recorded: patient characteristics, prostate volume in cubic centimeters estimated by TRUS about 1 month before the procedure, the number of needles, the number of seeds implanted, the operating time, and the status (presence or absence) of PAI during implantation.

Statistical analysis

To test for significant differences among patients with and without seed migration, variables in these groups were compared using the Mann–Whitney U test. The χ^2 test was used for categorical data. A value of $p < 0.05$ was considered statistically significant. Data are presented as the mean ± standard error (SE) or number of patients, according to the variables.

The significance of variables for predicting seed migration was assessed based on receiver operating characteristic (ROC) curves, which are plots of the true positive rate (sensitivity) vs. the false-positive rates (1-specificity) using all possible cutoff values. To estimate the predictive value of the variables, the area under the curve (AUC) was calculated and compared as described by Hanley and McNeil (9).

Independent predictors of seed migration were identified by multivariate stepwise logistic regression analysis. The predicted probability of seed migration (p) was estimated using the formula, $p = 1/(1 + \exp[-k])$. Logistic regression produces a score of k, where $k = a + b_1X_1 + b_2X_2 + \cdots$, which is a linear combination of the predictors (X_1, X_2,...)

Table 1
Characteristics of all patients stratified by results of seed migration

	Results of seed migration			
	Total (n = 158)	Seed migration (−) (n = 123)	Seed migration (−) (n = 35)	P value
Age (years)	68.7 ± 0.5	68.7 ± 0.6	68.6 ± 1.2	0.883
Initial PSA (ng/ml)	7.12 ± 0.25	7.10 ± 0.29	7.19 ± 0.48	0.621
TRUS preoperative prostate volume (cc)	23.3 ± 0.5	22.4 ± 0.5	26.3 ± 1.0	0.001
Number of needles	25.7 ± 0.4	24.9 ± 0.5	28.2 ± 0.9	0.002
Number of seeds implanted	71.1 ± 1.0	69.2 ± 1.1	77.9 ± 2.0	<0.001
Operating time (min)	65.0 ± 2.3	63.4 ± 2.3	70.7 ± 6.5	0.291
Gleason score				
<7	126	100	26	0.474
≥7	32	23	9	
NHT				
Yes	68	54	14	0.704
No	90	69	21	
PAI				
Yes	18	9	9	0.005
No	140	114	26	

Data presented as mean ± SE or n.

PSA, prostate-specific antigen; SE, standard error of the mean; TRUS, transrectal ultrasound; ; NHT, neoadjuvant hormonal therapy; PAI, pubic arch interference.

in the model. The model coefficients ($a, b_1, b_2, \ldots$) were chosen to optimize the model's ability to predict the probability of seed migration.

Results

Seed migration occurred in 35 (22.2%) of 158 patients. In 27 (77.1%) of the 35 patients, only a single seed migrated. In the remaining 8 (22.9%) patients, two or three seeds migrated. A total of 46 of 11,240 implanted seeds migrated. Thirty-three (0.294%) migrated to the lungs, more commonly to the left lung. Three (0.0267%) migrated to the abdomen. Ten (0.0890%) migrated to the pelvis. A series of radiographs were obtained at 3.6 ± 0.048 months (mean $\pm$ SE).

Table 1 shows the results of univariate analysis in all 158 patients. The preoperative prostate volume estimated by TRUS, the number of needles, and the number of seeds implanted were significantly higher in patients with seed migration than in those without. These results indicated that larger prostate glands were more likely to have seed migration. However, the absolute difference in prostate size was not overly impressive (22.4 vs. 26.3 cm^3). There were no significant differences in patient age, prostate-specific antigen (PSA), and operating time between patients with seed migration and those without. Seed migration was found in 9 (50.0%) of the 18 patients with PAI during implantation and in 26 (18.6%) of the remaining 140 patients without. The presence of PAI was associated significantly with seed migration, but neoadjuvant hormonal therapy (NHT) and Gleason score (≥ 7 vs. <7) were not.

The calculated AUC $\pm$ SE was 0.508 ± 0.058 for age, 0.528 ± 0.052 for initial PSA, 0.679 ± 0.049 for preoperative prostate volume by TRUS, 0.668 ± 0.052 for the number of needles, 0.693 ± 0.051 for the number of seeds implanted, and 0.559 ± 0.050 for operating time in all 158 patients. The number of seeds implanted had the largest AUC of all six continuous variables. However, there were no significant differences in AUC based on the preoperative prostate volume, the number of needles, and the number of seeds implanted. Figure 1 demonstrates the ROC curves for the preoperative prostate volume, the number of needles, and the number of seeds implanted.

Stepwise logistic regression analysis for the prediction of seed migration with these variables showed that the number of seeds implanted ($p = 0.001$) and the presence or absence of PAI ($p = 0.012$) were significant independent predictors. The probability for seed migration was calculated with the logistic regression formula with the number of seeds implanted and the presence or absence of PAI as parameters. The logistic regression equation is: $p = 1/(1 + \exp[6.074 - 0.063X_1 - 1.368X_2])$, where X_1 is the number of seeds implanted, $X_2 = 1$ if PAI is present, and $X_2 = 0$ if PAI is absent. Figure 2 shows the calculated logistic curves for the number of seeds implanted combined with the presence or absence of PAI for the prediction of seed migration.

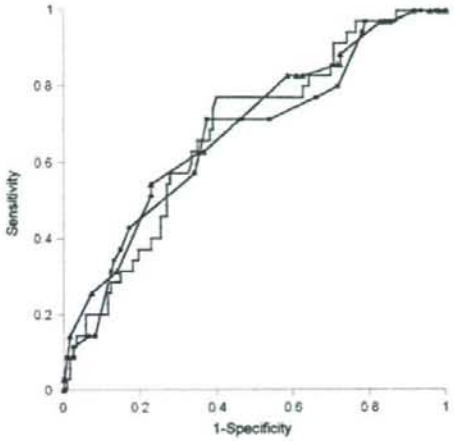

Fig. 1. Receiver operating characteristic curve analyses of preoperative prostate volume (+), the number of needles (■), and the number of seeds implanted (▲). Data are shown for all 158 patients.

Discussion

The purpose of the present study was to determine the incidence and predictors of seed migration after transperineal interstitial prostate brachytherapy using I-125 free seeds. The incidence of seed migration in the present study was similar to those previously reported (1–4). The overall seed embolization rate of implanted seeds was 0.409% (46/11,240), which is also consistent with previous reports (4, 6, 10–13). Univariate analyses demonstrated that the preoperative prostate volume estimated by TRUS, the number of needles, the number of seeds implanted, and the presence or absence of PAI were associated significantly with seed migration in all 158 patients. Multivariate logistic regression analysis, however, demonstrated that only the number of seeds implanted and the presence or absence of PAI were significant independent predictors of seed migration.

Some investigators have reported that the number of seeds implanted was a useful predictor of seed migration after transperineal interstitial prostate brachytherapy, and the result of the present study is consistent with those findings (10). However, other investigators have reported different results (11, 12). Eshleman et al. have reported that the number of seeds extraprostatically planned was a statistically significant predictor of seed migration (11). On the other hand, Fuller et al. have reported that source type (stranded vs. free) was a statistically significant predictor of seed migration (12).

The discrepancy in results seems due to several factors. First, seed placement differed among investigators. Some investigators have routinely placed several seeds extraprostatically to cover the periprostatic area, whereas other investigators have not. Second, source type (stranded vs.

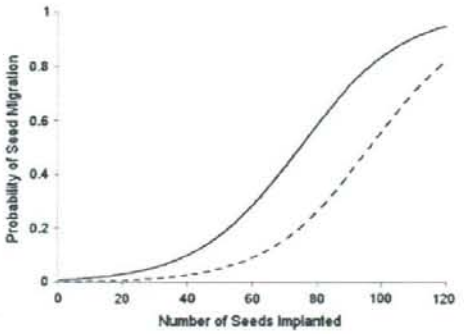

Fig. 2. The calculated logistic curves for the number of seeds implanted and the presence or absence of PAI for the prediction of seed migration. Solid line, PAI; dashed line, no PAI.

free) differed among investigators. Third, examined sites of seed migration differed among investigators. Some investigators limited their study to the pulmonary migration of implants, whereas other investigators examined seeds that migrated to the abdomen and the pelvis as well as the chest. Finally, some investigators might have underestimated the incidence of pulmonary seed migration, because not all of them reviewed a lateral view of the chest radiographs. Merrick et al. reported that 10% to 15% of patients with pulmonary seeds would go undiagnosed without a lateral view of the chest (13).

In the present study, extraprostatic seed placement was not intentionally undertaken, and no linked seeds were used. Furthermore, orthogonal chest radiographs, a KUB radiograph, and a posteroanterior pelvic radiograph were obtained and reviewed for all 158 patients to examine seeds migrated to the chest, the abdomen, and the pelvis, respectively. Under these circumstances, the number of seeds implanted is considered to be a significant independent predictor of seed migration.

The presence of PAI was also demonstrated to be a significant independent predictor of seed migration after transperineal interstitial prostate brachytherapy. To our knowledge, this is the first report of such an association. The reason the occurrence of PAI may increase the risk of seed migration is unclear. We hypothesize that the risk of seed migration may be associated with seed misplacement caused by oblique needle insertion due to PAI. Patients with PAI cannot be treated with the current brachytherapy techniques using parallel needle trajectories guided by a fixed template, because the posterior aspect of the pubic arch blocks the access of the needle to the anterior or anterolateral aspect of the prostate (14). If PAI is small, it will be overcome, and parallel needle insertion will be possible by performing various manipulations, which include angling the probe tip more anteriorly before the initial needle insertion or using the more extended lithotomy position to better expose the prostate from behind the pubic arch. However, when PAI is not solved by these manipulations, oblique needle insertion using a more inferior or medial hole of the template than that planned will be needed (14).

It has been reported that oblique needle insertion during brachytherapy can lead to errors in determining needle tip position and subsequent seed misplacement (15). This is because oblique needle insertion will result in the needle intersecting the two-dimensional TRUS image plane; thus, the needle will appear only as a dot in this image (14). If the needle does not appear as a line by TRUS, the spatial configuration of the tip of the needle and the boundary of the prostate base or apex will not be fully recognized. Under these conditions, seeds may not be placed accurately in their intended positions, and may sometimes be placed erroneously outside the prostatic capsule. Seeds placed outside the prostate could have access to the prostatic venous plexus and migrate to other sites. Thus, we hypothesize that the risk of seed migration may be associated with seed misplacement caused by oblique needle insertion due to PAI. However, there is no evidence for this hypothesis at present. Moreover, an underlying problem remains unsolved with this hypothesis: in the 9 patients with PAI during implantation and subsequent seed migration, it has still not been determined whether the migrated seeds had been released from the needle obliquely inserted due to PAI. Much more research will be needed to support this hypothesis.

In the present study, the incidence of PAI was lower than those in previous studies, in which it ranged from 19% to 29% (16, 17). This is because PAI was judged to be present only when it was not solved by the manipulations, and oblique needle insertion was undertaken through a more inferior or medial hole of the template than that planned. It is also because NHT for downsizing the prostate was undertaken to avoid PAI if substantial PAI was suspected at the preimplant volume study by TRUS. Because there were a limited number of patients with PAI in the present study, a larger series with more patients will be anticipated to confirm the importance of PAI for predicting seed migration.

Conclusion

The results of the present study showed that the number of seeds implanted and the presence or absence of PAI provided the most predictive information on seed migration in patients who underwent transperineal interstitial prostate brachytherapy. Thus, the combination of these two factors can be used to predict the risk of seed migration.

References

[1] Blair HF, Porter A, Chen QS. In vivo detection of an ^{125}I seed located in the intracardiac region after prostate permanent brachytherapy. *Int J Radiat Oncol Biol Phys* 2004;58:888–891.

[2] Davis BJ, Bresnahan JF, Stafford SL, *et al.* Prostate brachytherapy seed migration to a coronary artery found during angiography. *J Urol* 2002;168:1103.

[3] Davis BJ, Pfeifer EA, Wilson TM, *et al.* Prostate brachytherapy seed migration to the right ventricle found at autopsy following acute cardiac dysrhythmia. *J Urol* 2000;164:1661.

[4] Kunos CA, Resnick MI, Kinsella TJ, *et al.* Migration of implanted free radioactive seeds for adenocarcinoma of the prostate using a Mick applicator. *Brachytherapy* 2004;3:71–77.

[5] Older RA, Synder B, Krupski TL, *et al.* Radioactive implant migration in patients treated for localized prostate cancer with interstitial brachytherapy. *J Urol* 2001;165:1590–1592.

[6] Stone NN, Stock RG. Reduction of pulmonary migration of permanent interstitial sources in patients undergoing prostate brachytherapy. *Urology* 2005;66:119–123.

[7] Sommerkamp H, Rupprecht M, Wannenmacher M. Seed loss in interstitial radiotherapy of prostatic carcinoma with I-125. *Int J Radiat Oncol Biol Phys* 1988;14:389–392.

[8] Nath R, Anderson LL, Luxton G, *et al.* Dosimetry of interstitial brachytherapy sources: recommendations of the AAPM Radiation Therapy Committee Task Group No. 43. American Association of Physicists in Medicine. *Med Phys* 1995;22:209–234.

[9] Hanley JA, McNeil BJ. A method of comparing the areas under receiver operating characteristic curves derived from the same cases. *Radiology* 1983;148:839–843.

[10] Ankem MK, DeCarvalho VS, Harangozo AM, *et al.* Implications of radioactive seed migration to the lungs after prostate brachytherapy. *Urology* 2002;59:555–559.

[11] Eshleman JS, Davis BJ, Pisansky TM, *et al.* Radioactive seed migration to the chest after transperineal interstitial prostate brachytherapy: extraprostatic seed placement correlates with migration. *Int J Radiat Oncol Biol Phys* 2004;59:419–425.

[12] Fuller DB, Koziol JA, Feng AC. Prostate brachytherapy seed migration and dosimetry: analysis of stranded sources and other potential predictive factors. *Brachytherapy* 2004;3:10–19.

[13] Merrick GS, Butler WM, Dorsey AT, *et al.* Seed fixity in the prostate/periprostatic region following brachytherapy. *Int J Radiat Oncol Biol Phys* 2000;46:215–220.

[14] Wei Z, Gardi L, Downey DB, *et al.* Oblique needle segmentation and tracking for 3D TRUS guided prostate brachytherapy. *Med Phys* 2005;32:2928–2941.

[15] Wan G, Wei Z, Gardi L, *et al.* Brachytherapy needle deflection evaluation and correction. *Med Phys* 2005;32:902–909.

[16] Sejpal S. Intraoperative pubic arch interference (i-PAI) during transrectal ultrasound guided prostate seed brachytherapy (PB) in patients with CT-based prostate to pubic-arch overlap (PAO) of ≤1 cm. *Int J Radiat Oncol Biol Phys* 2007;69:S379–S380.

[17] Strang JG, Rubens DJ, Brasacchio RA, *et al.* Real-time US versus CT determination of pubic arch interference for brachytherapy. *Radiology* 2001;219:387–393.

Int. J. Radiation Oncology Biol. Phys., Vol. 73, No. 1, pp. 80–87, 2009

0360-3016/09/$–see front matter

ELSEVIER

doi:10.1016/j.ijrobp.2008.04.003

CLINICAL INVESTIGATION **Breast**

DOSE DISTRIBUTION ANALYSIS OF AXILLARY LYMPH NODES FOR THREE-DIMENSIONAL CONFORMAL RADIOTHERAPY WITH A FIELD-IN-FIELD TECHNIQUE FOR BREAST CANCER

TOSHIO OHASHI, M.D.,* ATSUYA TAKEDA, M.D.,† NAOYUKI SHIGEMATSU, M.D.,* JUNICHI FUKADA, M.D.,* NAOKO SANUKI, M.D.,† ATSUSHI AMEMIYA, M.D.,‡ AND ATSUSHI KUBO, M.D.*

*Department of Radiology, Keio University, School of Medicine, Tokyo, Japan; †Department of Radiology, Ofuna Chuo Hospital, Kanagawa, Japan; and ‡Department of Surgery, Ofuna Chuo Hospital, Kanagawa, Japan

Purpose: We previously reported that most of axillary regions could be irradiated by the modified tangential irradiation technique (MTIT). The purpose of this study was to determine whether the three-dimensional conformal radiotherapy (3D-CRT) with a field-in-field technique improves dosimetry for the breast and axillary nodes.

Methods and Materials: Fifty patients with left-sided breast cancer were enrolled. With MTIT, we planned the radiation field to be wider in the cranial direction than the standard tangential fields to include the axillary regions. With 3D-CRT, a field-in-field technique was used to spare the heart and contralateral breast to the extent possible by applying the multileaf collimator manually. Dose–volume histograms were compared for the breast, axillary region, heart, lung, and other normal tissues.

Results: There were no significant differences in the percent volume of the breast receiving >90% of the prescribed dose (V90) between MTIT and 3D-CRT. The mean V90 of the level I to III axillary regions were increased from 93.7%, 48.2%, and 41.3% with MTIT to 97.6%, 85.8%, and 82.8% with 3D-CRT. 3D-CRT significantly reduced the volume of the heart receiving >30 Gy (mean, 7.6 vs. 15.9 mL), the percent volume of the bilateral lung receiving >20 Gy (7.4% vs. 8.9%), and the volume of other normal tissues receiving >107% of the prescribed dose (0.1 vs. 2.9 mL).

Conclusion: The use of 3D-CRT with a field-in-field technique improves axillary node coverage, while decreasing doses to the heart, lungs, and the other normal tissues, compared with MTIT.

Breast cancer, Axillary node, Radiotherapy, Three-dimensional conformal radiotherapy, Dose–volume histogram.

INTRODUCTION

The role of routine axillary dissection in the management of localized breast cancer is controversial (1–3). Performing axillary radiotherapy without axillary dissection or with only sentinel node biopsy is an option for clinically node-negative patients (4–10). When radiation therapy is used as a primary axillary treatment modality or after sentinel node biopsy, the axilla is usually intact or minimally altered. Irradiation of the regional lymph nodes remains an important but technically challenging part of the management of breast cancer.

The traditional standard tangential fields include the lowest part of the axilla but fail to deliver therapeutic doses to any of the three axillary levels. As we previously reported (11, 12), it is possible to cover almost the entire axillary lymph node region using the modified tangential irradiation technique (MTIT) on the basis of fluoroscopic simulation or planning without three-dimensional (3D) data, although the doses delivered to some areas are not adequate.

Recently, 3D conformal tangential radiotherapy and intensity-modulated radiotherapy (IMRT) using CT-based planning have been applied in an effort to improve the local control rate and reduce toxicity (13–15). Fifteen-year cardiac mortality was higher for patients who received radiotherapy for left-sided compared with right-sided breast cancer (16–19) or after radiotherapy for Hodgkin's disease (20), presumably because of irradiation to cardiac structures.

At Ofuna Chuo Hospital, instead of the traditional standard tangential technique, we have been using 3D conformal radiotherapy (3D-CRT) with a static field-in-field technique for breast cancer. In this study, we carried out a comparative treatment-planning study to determine whether the use of 3D-CRT with a field-in-field technique improves dosimetry for the breast and regional lymph nodes.

Reprint requests to: Toshio Ohashi, M.D., Department of Radiology, Keio University, School of Medicine, 35 Shinanomachi, Shinjuku-ku, Tokyo 160-8582, Japan. Tel: (+81) 3-3353-1211; Fax: (+81) 3-3359-7425; E-mail: ohashi@rad.med.keio.ac.jp

Conflict of interest: none.

Received March 15, 2008, and in revised form April 8, 2008. Accepted for publication April 9, 2008.

Table 1. Patient characteristics

	n (%)	Median (Range)
Age (years)	—	56 (29–84)
T stage	—	—
T1	29 (58%)	—
T2	20 (40%)	—
T3	1 (2%)	—
Pathology		
Invasive ductal carcinoma	48 (96%)	—
Invasive lobular carcinoma	1 (2%)	—
Mucinous carcinoma	1 (2%)	—
Chemotherapy	8 (16%)	—
Hormone therapy	30 (60%)	—
Volume (mL)		
Breast	—	314.4 (116.4–1445.5)
LN level I	—	48.1 (14.9–106.2)
LN level II	—	7.9 (2.6–21.2)
LN level III	—	2.7 (0.4–9.3)
RN	—	3.2 (0.4–6.7)
SLN	—	4 (1.7–20.4)

Abbreviations: LN = lymph node; RN = Rotter's node; SLN = sentinel lymph node.

METHODS AND MATERIALS

Patients

The subjects were 50 consecutive patients undergoing breast-conserving surgery for left-sided breast cancer at Ofuna Chuo Hospital. Patient characteristics are shown in Table 1. All patients were clinically node-negative and received sentinel lymph node (SLN) biopsy without axillary dissection. During the SLN biopsy, surgical clips were left in place as markers.

Each patient was immobilized in the both arms-up position during treatment. A planning CT scan at 5-mm intervals was obtained at the same position, and the CT data were transferred into the CMS XiO treatment system via a network connection.

Delineation of target and organ at risk

The clinical target volume (CTV) included the whole breast and the level I to II axillary nodal regions. The breast contour was defined medially at the lateral edge of the sternum, inferiorly at the inframammary fold, superiorly at the inferior edge of the medial head of the clavicle, and laterally to include all apparent breast tissue, referring to the area exhibiting greater density than the surrounding fatty tissue.

The axillary nodal region was divided into levels I to III, Rotter's nodes (RN), and the SLN (Fig. 1). The level I region was defined as the area lateral to the lateral border of the pectoralis minor muscle and extending superiorly to the level of the axillary vein. The level II region was defined as the area between the medial and lateral borders of the pectoralis minor muscle, extending superiorly to the level of the axillary vein. The level III region was defined as the area medial to the medial margin of the pectoralis minor muscle and adjacent to the chest wall, extending superiorly to the level of the axillary vein. The RN region was defined as the area between the pectoralis major and pectoralis minor muscles. The SLN region was defined as the area within 5 mm of the surgical markers. The inferior border of the axilla was defined as being located at the level between the fourth and fifth thoracic ribs (21).

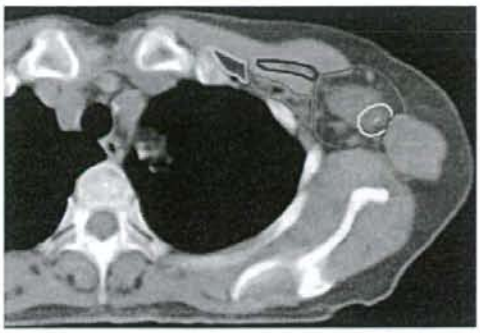

Fig. 1. An example of computed tomography image showing the axillary lymph node region. Level I is shown in red, level II in pink, level III in light blue, Rotter's node region in blue, surgical clip in green, and the sentinel lymph node region in yellow.

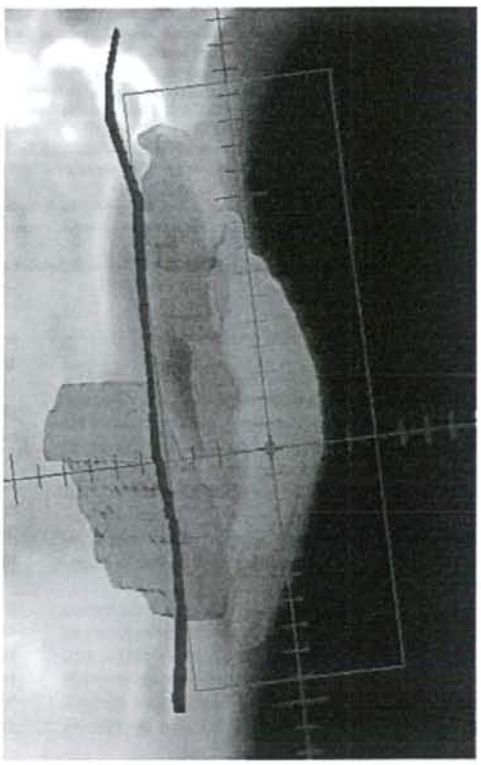

Fig. 2. Digitally reconstructed radiograph for a typical modified tangential irradiation technique. Breast planning target volume is shown in pink, axillary nodal planning target volume in green, the heart in red, and the midsternal line in blue.

Posteriorly, the CTV was the junction of the breast tissue and chest wall or pectoralis major muscle. Anteriorly, the CTV was parallel to but 3 mm below the surface of the skin, which was intended to reduce underestimation due to the built-up effect. The planning target volume (PTV) was defined as the CTV with 3-mm margins, except for the skin area.

The heart, both lungs, and other normal tissues such as the skin and soft tissue were contoured as the organ at risk.

Treatment planning techniques

The superposition algorithm was used for dose calculations in all treatment plans. The prescribed dose to the PTV was 50 Gy, delivered in 2- Gy fractions. Two plans were devised for each patient. The first was the aforementioned MTIT plan, also described in our previous study (11, 12). In brief, the radiation field size was planned to be wider in the cranial and posterior directions than the traditional standard tangential fields to ensure inclusion of the axillary regions (Fig. 2). In most cases, the field from the anterior oblique view covers one half of the humeral head in digitally reconstructed radiographs created from the CT information, and the collimator angle for MTIT was somewhat steeper than that of the traditional standard tangential plan. The latter modification was made to decrease the lung volume that was irradiated. The physical wedge angles and relative weights of beams are optimized to provide dose uniformity to the maximum extent possible.

Our second approach was the 3D-CRT plan with or without a field-in-field technique. The isocenter was selected to be at approximately the center of the PTV. The gantry angles for the tangential fields were similar to those of MTIT and were selected with the aid of digitally reconstructed radiographs. A leaf margin of 1 cm to the PTV was added, without collimator rotations, in all directions except ventral and dorsal. To the leaf margin of the ventral side of the fields, 2 cm were added to ensure coverage of the breast surface. The dorsal sides of the fields were arranged to avoid the heart unless there was overlap with the tumor bed and not to exceed the midsternal line, by manually applying the multileaf collimators (Fig. 3A). We set the weight point around the center of the PTV and confirmed that the dorsal edge of the breast tissue was covered within the prescribed 95% isodose. The physical wedge angles and relative weights of beams were optimized to provide dose uniformity.

However, some patients received a dose exceeding 107% of the prescribed dose, that is, to a "hot" region (Fig. 3B). In patients with these hot regions, we used a field-in-field technique to reduce dose inhomogeneity. The weight of the original set of fields is reduced (usually 90%–95%) so that the hot regions receive the prescribed dose. The second set of fields has the same beam parameters but is designed to avoid the hot region, and the weight is typically approximately 10% of the total dose (Fig. 3C).

Dose evaluation and statistical analysis

Dose–volume histograms (DVHs) were calculated for the breast, axillary nodal region (levels I to III, RN, and SLN), the heart, the lungs, and other normal tissues. The breast and axillary nodal region were compared on the basis of the percent volumes receiving more than 90%, 95%, and 107% of the prescribed dose (V90, V95, and V107, respectively) and homogeneity. The homogeneity index (HI) was defined as the fraction with a dose between 95% and 107% of the prescribed dose.

Normal treated tissues were compared on the basis of the heart volume receiving more than 40 Gy and 30 Gy (V40 Gy and V30 Gy, respectively), the percentage of bilateral lung volumes receiving more than 20 Gy (V20 Gy), and other normal tissue volumes receiving more than 107% of the prescribed dose. Comparisons were made using the paired t test (two-sided) for each evaluation parameter. Analyses were carried out using SPSS 15.0 (SPSS, Chicago, IL). Differences were regarded as statistically significant at p values of less than 0.05.

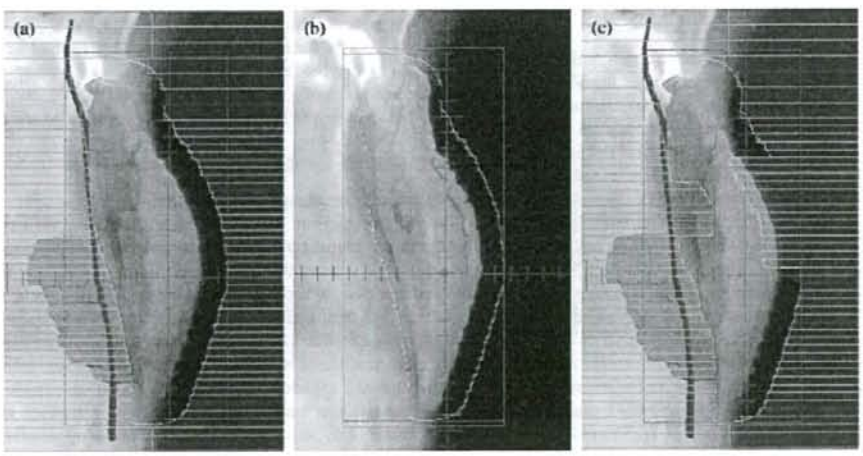

Fig. 3. Three-dimensional conformal radiotherapy with a field-in-field technique. (a) The original set field. The dorsal side was arranged to avoid irradiating the heart, unless there was overlap with the tumor bed, and not to exceed the midsternal line. (b) A hot region receiving >107% is shown in orange for the original set field. The 95% isodose area is shown in brown. (c) The second set field was designed to avoid the hot region. The weight is typically approximately 10% of the total dose.

Table 2. Dosimetric characteristics of the breast and axillary regions for each technique

Structure	Parameters	Mean (95% CI) 3D-CRT	Mean (95% CI) MTIT	*p* value
Breast	V90 (%)	96.1 (95.7–96.5)	96.9 (96.3–97.4)	0.28
	V95 (%)	87.2 (85.9–88.5)	88.3 (86.7–89.9)	0.2
	V107 (%)	0 (0–0.05)	0.2 (0.08–0.31)	<0.01
	HI	0.87 (0.86–0.89)	0.89 (0.87–0.90)	0.22
Axillary region				
Level I	V90 (%)	97.6 (96.0–99.2)	93.7 (91.3–96.0)	<0.01
	V95 (%)	87.0 (82.3–91.8)	59.6 (53.1–66.0)	<0.01
	V107 (%)	0 (0–0)	0.5 (0–1.2)	0.2
	HI	0.92 (0.88–0.95)	0.66 (0.58–0.74)	<0.01
Level II	V90 (%)	89.5 (84.2–94.7)	49.6 (38.3–68.9)	<0.01
	V95 (%)	34.7 (24.9–44.6)	9.1 (2.0–16.1)	<0.01
	V107 (%)	0 (0–0)	0 (0–0)	—
	HI	0.35 (0.25–0.45)	0.09 (0.02–0.2)	<0.01
Level III	V90 (%)	85.8 (78.5–93.2)	41.7 (28.1–55.3)	<0.01
	V95 (%)	40.7 (26.4–55.0)	5.1 (0.1–10.2)	<0.01
	V107 (%)	0 (0–0)	0 (0–0)	—
	HI	0.41 (0.26–0.55)	0.05 (0–0.10)	<0.01
RN	V90 (%)	96.6 (89.5–100)	94.7 (90.5–98.9)	0.63
	V95 (%)	93.8 (86.3–100)	47.6 (33.5–61.7)	<0.01
	V107 (%)	0 (0–0.1)	0 (0–0.1)	0.32
	HI	0.94 (0.86–1.0)	0.48 (0.34–0.62)	<0.01
SLN	V90 (%)	99.8 (99.6–100)	99.6 (99.1–100)	0.08
	V95 (%)	98.5 (96.5–100)	83.1 (73.3–92.8)	<0.01
	V107 (%)	0 (0–0)	0.1 (0–0.2)	0.16
	HI	0.98 (0.96–1.0)	0.83 (0.73–0.93)	<0.01

Abbreviations: CI = confidence interval; HI = homogeneity index; MTIT = modified tangential irradiation technique; RN = Rotter's node; SLN = sentinel lymph node; 3D-CRT = Three-dimensional conformal radiotherapy.

RESULTS

The median volumes of the breast, axillary levels I, II, III, RN, and SLN are shown in Table 1. In 40 patients (80%), a field-in-field technique was used in 3D-CRT to reduce dose inhomogeneity. The planning time for 3D-CRT at the computer was 30 min on average.

The dosimetric parameters of the breast and axillary regions are shown in Table 2. The variability of the V90 and V95 values in the breast and axillary regions are shown in Fig. 4. In V90, V95, and HI of the breast, there were no significant differences between 3D-CRT and MTIT. The mean values of levels I to III nodal V90 and V95 increased significantly with 3D-CRT, compared with MTIT. However, the mean values of levels II and III nodal V95 with 3D-CRT were 34.7% and 40.7%, respectively, suggesting inadequate coverage even with 3D-CRT. The mean values of RN and SLN V95 in 3D-CRT indicated excellent coverage values of 93.8% and 98.5%, respectively, vs. only 47.6% and 83.1% with MTIT.

The dosimetric parameters for the heart, lungs, and the other normal tissues are shown in Table 3. The entire organ at risk showed reduced doses with the 3D-CRT plan compared with MTIT (all parameters: $p < 0.01$). The maximum value of V107 for the other normal tissues was 25.1 mL with MTIT. In contrast, with 3D-CRT the V107 of the other normal tissues was less than 1 mL in all patients.

Among all 50 patients, 35 (70%) and 14 (28%) required a physical wedge for MTIT and 3D-CRT, respectively, to administer an adequate dose. In 24 of the 35 patients needing a physical wedge for MTIT, an acceptable 3D-CRT plan was feasible without using a physical wedge. The total monitor unit (MU) was decreased a mean of 10.3% in these 24 patients (mean, MTIT vs. 3D-CRT, 295.6 vs. 264.8 MU; $p < 0.01$). Only three patients required a physical wedge for 3D-CRT planning and none for MTIT. In the other 23 patients, there was no difference between the two plans in terms of whether a wedge was necessary. There were no significant differences in total MU between MTIT and 3D-CRT in these 23 patients.

DISCUSSION

Significance of irradiation to the axilla

Various alternatives to axillary node dissection are currently being investigated, including axillary lymph node sampling, SLN dissection, and primary radiation therapy of the nodal region. In these situations, when radiation therapy is intended to treat axillary tissues, applying an appropriate technique is important to minimize locoregional recurrence rates. The traditional standard tangential irradiation technique is usually applied to patients with breast cancer after breast-conservation therapy and is expected to irradiate all breast tissue and, to some extent, the low-lying axillary lymph node regions (11, 12, 22–25).

We looked at surgical axillary clip placement in 63 patients in relation to standard tangential fields and recommended significant modifications of the standard tangential fields, or MTIT, to include these clips (11). Using MTIT allowed

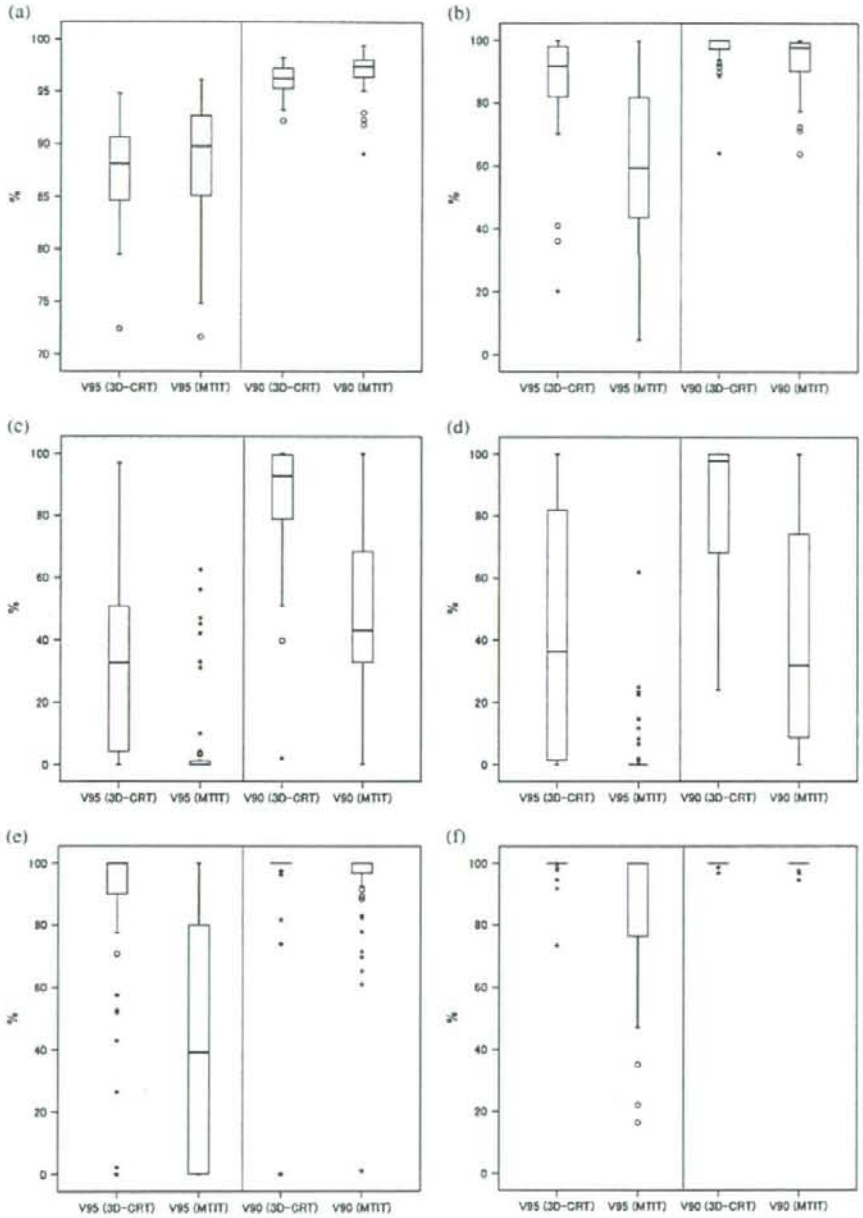

Fig. 4. Boxplots of the V90 and V95 values in the breast and axillary regions. (a) Breast, (b) Lymph node (LN) level I, (c) LN level II, (d) LN level III, (e) Rotter's node, and (f) sentinel lymph node. The lowest and highest 10% of the data are shown as points beyond the error bars. The box includes the central 50% of the data (25%–75%). The solid line within each box is the median of the data.

Table 3. Dosimetric characteristics of the organ at risk for each technique

Structure	Parameters	Mean (95% CI) 3D-CRT	Mean (95% CI) MTIT	*p* value
Heart	V30 Gy (mL)	7.6 (5.1–10.2)	15.9 (11.3–20.6)	<0.01
	V40 Gy (mL)	4.4 (2.5–6.3)	10.6 (6.9–14.4)	<0.01
Lungs	V20 Gy (%)	7.4 (6.6–8.2)	8.9 (8.1–9.7)	<0.01
Other normal tissues	V107 (mL)	0.1 (0–0.3)	2.9 (1.3–4.4)	<0.01

Abbreviations: 95% CI = 95% confidence interval; MTIT = modified tangential irradiation technique; 3D-CRT = Three-dimensional conformal radiotherapy.

axillary nodal coverage to be improved, but the median V80% of axillary region levels I and II were 90% and 81%, an apparently insufficient dose to control axillary lymph node recurrence (12). Some studies have described modified tangential fields including the axillary region, but few reports have compared axillary coverage based on DVH between modified tangential fields and traditional standard fields. Reznik *et al.* (22) demonstrated that when modified tangential fields are applied, coverage improves significantly, but the average dosages received by the axillary regions are still less than 90% of the prescribed dose. It was also reported that 79% of level I, 51% of level II, and 49% of level III received 95% of the prescribed dose with modified tangential fields (22). These findings were consistent with those of our previous studies (12).

In this study, the dosimetric investigation with 3D-CRT demonstrated the feasibility of improved breast and nodal target coverage without excessive doses to normal tissue or an unreasonable increase in the complexity of treatment delivery, compared with MTIT. However, because the axillary region is farther from the skin surface than the breast depending on the direction of the incident beam, dose reduction can occur in the deep aspect of the axillary region, primarily in the posterior-superior region of the axilla, compared with the breast. Therefore, 95% isodose line coverage of the axillary region is frequently difficult, despite an increase in V90.

The use of IMRT may even produce greater improvements in the dose distribution. Dogan *et al.* (26) found the use of IMRT to improve breast and regional node coverage, compared with conventional 3D-CRT techniques and the nine-field IMRT technique provided satisfactory doses to the axillary nodes (the mean value of the minimal dose received by 95% of the axillary nodes was 50.3 Gy with a prescription of 50 Gy). However, these improvements were achieved at the expense of extra doses to the esophagus and thyroid.

Irradiation to organ at risk

The 3D-CRT approach with a field-in-field technique resulted in a modestly higher dose to adjacent healthy tissues. Minimizing the heart dose is a concern for left-sided breast cancer patients. Previous studies of early-stage breast cancer (27) and Hodgkin's lymphoma (28) have shown that, if the heart receives <30 Gy, cardiac complications are likely to be minimal. This study showed that while maintaining excellent breast and regional node coverage, all 3D-CRT plans significantly reduced the dose to the heart. The 3D-CRT plan usually excludes the heart from the irradiation field, unless the tumor bed overlaps the heart, which may reduce V95 for the breast. Some reports have described partial breast radiotherapy as achieving acceptable 5-year rates of breast tumor control and suggested that it is often not necessary to treat the whole breast (29–31). The effect on overall survival of comprehensive partial breast radiotherapy, while avoiding an excess risk of myocardial injury, awaits long-term follow-up.

Pneumonitis rates in breast cancer patients treated with standard tangential fields are usually low and are thus clinically acceptable (32). Including the axillary region in the target volume increases the lung volume irradiated (11, 12), and this may increase the probability of pneumonitis in some patients (33). However, in this study, V20 Gy and DVHs of the lung for all patients were acceptable. The main concern with healthy tissue dose increases of this magnitude is an increased risk of late secondary malignancy (34, 35). This is likely to be of greatest concern in younger women and in patients with a low risk for systemic relapse who are likely to live for many decades after the diagnosis of breast cancer. There have been reports that adjuvant radiotherapy for breast cancer may increase the risks of lung cancer and angiosarcoma (36, 37). Balancing the short- to medium-term benefits of reducing the heart and left lung volumes receiving a high dose of radiotherapy against the risk of later malignancy requires an individual assessment of the treatment volume goals and the patient's longevity prospects.

Also, the risk of developing brachial plexopathy after conventional radiotherapy with a total dose 50 Gy, with 2 Gy per fraction to the breast is estimated to be less than 1% (38, 39). Adequate irradiation of the axillary region in 3D-CRT may be associated with an increased risk of radiation-induced brachial plexopathy. Longer-term follow-up is necessary to determine whether our 3D-CRT technique is associated with an increased risk of brachial plexopathy.

Use of physical wedges

Woo *et al.* (40) reported that the dose of scattered radiation delivered to a patient's body is consistent with the exposures reported to be associated with excessive leukemia incidence and that the use of a physical wedge as compensation was the

most significant factor associated with an increase in the scattered dose.

The use of a physical wedge ensures a 95% isodose line coverage of the breast by increasing the doses to the lateral sides of the breast, while reducing the dose around the top of the breast. On the contrary, when the wedge is not used, the dose increases at the top of the breast but decreases on the lateral sides of the breast, precluding a 95% isodose line coverage of the breast. However, because 3D-CRT with a field-in-field technique sets the MU to cover the dorsal edge of the breast within the 95% isodose employing a beam without using wedges, the hot region occurring around the top of the breast can be blocked in the second set field, ultimately leading to an increase in dose homogeneity. Thus 3D-CRT with a field-in-field technique is frequently capable of preparing a homogeneous dose distribution within the PTV without using physical wedges. This has important implications for reducing MU, implementing treatment without precluding mechanical efficiency, and reducing the scattered dose.

CONCLUSION

The method presented here allows coverage of the breast tissue and axillary nodal regions up to 90%–95% of the prescribed dose using commonly available planning and treatment facilities. It is a widely applicable and clinically practical technique. Maintaining the same gantry angles for each set of multiple fields ensures that there is no increase in setup complexity and that treatments can be delivered quickly and reliably.

REFERENCES

1. Cady B. The need to reexamine axillary lymph node dissection in invasive cancer. *Cancer* 1994;73:505–508.
2. Haffty BG, Ward B, Pathare P, *et al.* Reappraisal of the role of axillary lymph node dissection in the conservative treatment of breast cancer. *J Clin Oncol* 1997;15:691–700.
3. Dent DM. Axillary lymphadenectomy for breast cancer: Paradigm shifts and pragmatic surgeons. *Arch Surg* 1996;131: 1125–1127.
4. Cady B, Stone MD, Wayne J. New therapeutic possibilities in primary invasive breast cancer. *Ann Surg* 1993;218:338–349.
5. Halverson KJ, Taylor ME, Perez CA, *et al.* Regional nodal management and patterns of failure following conservative surgery and radiation therapy for Stage 1 and 2 breast cancer. *Int J Radiat Oncol Biol Phys* 1993;26:593–599.
6. Hoskin PJ, Rajan B, Ebbs S, *et al.* Selective avoidance of lymphatic radiotherapy in the conservative management of early breast cancer. *Radiother Oncol* 1992;25:83–88.
7. Kuznetsova M, Graybill JC, Zusag TW, *et al.* Omission of axillary nymph node dissection in early-stage breast cancer: Effect on treatment outcome. *Radiology* 1995;197:507–510.
8. Ogawa Y, Nishioka A, Inomata T, *et al.* Conservation treatment intensified with tamoxifen and CAF chemotherapy without axillary dissection in cancer patients with clinically-negative axillary nodes. *Oncol Rep* 1999;6:801–805.
9. Wong JS, Recht A, Beard CJ, *et al.* Treatment outcome after tangential radiation therapy without axillary dissection in patients with early-stage breast cancer and clinically negative axillary nodes. *Int J Radiat Oncol Biol Phys* 1997;39:915–920.
10. Harlow SP, Krag DN. Sentinel lymph node—why study it: Implications of the B-32 study. *Semin Surg Oncol* 2001;20: 224–229.
11. Takeda A, Shigematsu N, Kondo M, *et al.* The modified tangential irradiation technique for breast caner: How to cover the entire axillary region. *Int J Radiat Oncol Biol Phys* 2000;46: 815–822.
12. Takeda A, Shigematsu N, Ikeda T, *et al.* Evaluation of novel modified tangential irradiation technique for breast cancer patients using dose-volume histogram. *Int J Radiat Oncol Biol Phys* 2004;58:1280–1288.
13. Thilmann C, Zabel A, Milker-Zabel S, *et al.* Number and orientation of beams in inversely planned intensity-modulated radiotherapy of the female breast and the parasternal lymph nodes. *Am J Clin Oncol* 2003;26:e136–e143.
14. Krueger EA, Fraass BA, McShan DL, *et al.* Potential gains for irradiation of chest wall and regional nodes with intensity modulated radiotherapy. *Int J Radiat Oncol Biol Phys* 2003;56: 1023–1037.
15. Beckham WA, Pepescu CC, Patenaude VV, *et al.* Is multibeam IMRT better than standard treatment for patients with left-sided breast cancer? *Int J Radiat Oncol Biol Phys* 2007;69:918–924.
16. Paszat LF, Mackillop WJ, Groome PA, *et al.* Mortality from myocardial infarction following postlumpectomy radiotherapy for breast cancer: A population-based study in Ontario, Canada. *Int J Radiat Oncol Biol Phys* 1999;43:755–762.
17. Paszat LF, Mackillop WJ, Groome PA, *et al.* Mortality from myocardial infarction after adjuvant radiotherapy for breast cancer in the surveillance, epidemiology, and end-results cancer registries. *J Clin Oncol* 1998;16:2625–2631.
18. Gyenes G, Rutqvist LE, Liedberg A, *et al.* Long-term cardiac morbidity and mortality in a randomized trial of pre- and postoperative radiation therapy versus surgery alone in primary breast cancer. *Radiother Oncol* 1998;48:185–190.
19. Cuzick J, Stewart H, Rutqvist L, *et al.* Cause-specific mortality in long-term survivors of breast cancer who participated in trials of radiotherapy. *J Clin Oncol* 1994;12:447–453.
20. Hancock SL, Tucker MA, Hoppe RT. Factors affecting late mortality from heart disease after treatment of Hodgkin's disease. *JAMA* 1993;270:1949–1955.
21. Harris JR, Lippman ME, *et al.* Diseases of the breast. 2nd ed. Philadelphia: Lippincott, Williams & Wilkins; 2000. p. 5–8, 404, 546–549.
22. Reznik J, Cicchetti MG, Degaspe B, *et al.* Analysis of axillary coverage during tangential radiation therapy to the breast. *Int J Radiat Oncol Biol Phys* 2005;61:163–168.
23. Aristei C, Chionne F, Marsella AR, *et al.* Evaluation of level I and II axillary nodes included in the standard breast tangential fields and calculation of the administered dose: Results of a prospective study. *Int J Radiat Oncol Biol Phys* 2001;51:69–73.
24. Reed DR, Lindsley SK, Mann GN, *et al.* Axillary lymph node dose with tangential breast irradiation. *Int J Radiat Oncol Biol Phys* 2005;61:358–364.
25. Schlembach PJ, Buchholz TA, Ross MI, *et al.* Relationship of sentinel and axillary level I–II lymph nodes to tangential fields used in breast irradiation. *Int J Radiat Oncol Biol Phys* 2001;51: 671–678.
26. Dogan N, Cuttino L, Lloyd R, *et al.* Optimized dose coverage of regional lymph nodes in breast cancer: The role of intensity-modulated radiotherapy. *Int J Radiat Oncol Biol Phys* 2007; 68:1238–1250.
27. Hortobagyi GN. Trastuzumab in the treatment of breast cancer. *N Engl J Med* 2005;353:1734–1736.
28. Weber DC, Ares C, Lomax AJ, *et al.* Radiation therapy planning with photons and protons for early and advanced breast cancer: An overview. *Radiat Oncol* 2006;1:22.

29. Polgar C, Sulyok Z, Fodor J, *et al.* Sole brachytherapy of the tumor bed after conservative surgery for T1 breast cancer: Five-year results of a Phase I–II study and initial findings of a randomized phase III trial. *J Surg Oncol* 2002;80:121–128.
30. Vicini FA, Baglan KL, Kestin LL, *et al.* Accelerated treatment of breast cancer. *J Clin Oncol* 2001;19:1993–2001.
31. Vicini FA, Remouchamps V, Wallace M, *et al.* Ongoing clinical experience utilizing 3D conformal external beam radiotherapy to deliver partial-breast irradiation in patients with early-stage breast cancer treated with breast-conserving therapy. *Int J Radiat Oncol Biol Phys* 2003;57:1247–1253.
32. Pierce SM, Recht A, Lingos TI, *et al.* Long-term radiation complications following conservative surgery (CS) and radiation therapy (RT) in patients with early stage breast cancer. *Int J Radiat Oncol Biol Phys* 1992;23:915–923.
33. Marks LB, Fan M, Clough R, *et al.* Radiation-induced pulmonary injury: Symptomatic versus subclinical endpoints. *Int J Radiat Biol* 2000;76:469–475.
34. Hall EJ, Wuu CS. Radiation-induced second cancers: The impact of 3D-CRT and IMRT. *Int J Radiat Oncol Biol Phys* 2003;56:83–88.
35. Gao X, Fisher SG, Emami B. Risk of second primary cancer in the contralateral breast in women treated for early-stage breast cancer: A population-based study. *Int J Radiat Oncol Biol Phys* 2003;56:1038–1045.
36. Roychoudhuri R, Evans H, Robinson D, *et al.* Radiation-induced malignancies following radiotherapy for breast cancer. *Br J Cancer* 2004;91:868–872.
37. Kirova YM, Gambotti L, De Rycke Y, *et al.* Risk of second malignancies after adjuvant radiotherapy for breast cancer: A large-scale, single-institution review. *Int J Radiat Oncol Biol Phys* 2007;68:359–363.
38. Fowble BL, Solin LJ, Schultz DJ, Goodman RL. Ten-year results of conservative surgery and irradiation for Stage I and II breast cancer. *Int J Radiat Oncol Biol Phys* 1991;21:269–277.
39. Pierce SM, Recht A, Lingos TI, *et al.* Long-term radiation complication following conservative surgery (CS) and radiation therapy (RT) in patients with early stage breast cancer. *Int J Radiat Oncol Biol Phys* 1992;23:915–923.
40. Woo TC, Pignol JP, Rakovitch E, *et al.* Body radiation exposure in breast cancer radiotherapy: Impact of breast IMRT and virtual wedge compensation techniques. *Int J Radiat Oncol Biol Phys* 2006;65:52–58.

トピックス

放射線治療の最前線
―高精度放射線治療―

国枝悦夫
久保敦司*

はじめに

人口の高齢化、生活習慣の変化に伴う癌患者の増加のみならず、他の治療法からの移行で、この10年間で放射線治療患者数は倍増しており、現在もますます増える傾向にある。乳癌の術後照射などに加えて、最近は前立腺癌の根治照射なども急増しているが、とくに最近の技術的な進歩として定位放射線治療、強度変調放射線治療で代表される高精度放射線治療の発展が著しい。

放射線治療の歴史は古く、X線の発見、ラジウムの発見の時代に遡る。その歴史のなかでは正常組織と腫瘍細胞の放射線感受性の差が最も重視されていた。すなわち化学療法と同様に、細胞増殖サイクルに働いて腫瘍細胞を選択的に抑え、細胞死に至らせる役割が放射線治療の根本原理とされていた。これは現在でも変わらないが、最近ではさらに3次元的な画像診断技術の発展に伴って、空間的に腫瘍分布に一致させ

て放射線を投与して、位置的に限局した腫瘍範囲を治療する、空間的な選別がより正確にできるようになってきた。

装置の進歩としては、ライナックはリアルタイムに照射野形状を変化させるマルチリーフコリメータや位置照合用イメージングシステムも搭載し、治療状態でのCT画像も撮影できるなど、ハードの発達も大きいが、治療計画から治療終了までのシステム全体の変化も著しい。

透視装置による位置決めの手順から患者CTデータを取り込んだワークステーションにて照射方向などの仮想的計画を行う3次元シミュレーションに依存する方法に大きく方向転換した。X線シミュレータ（透視装置）による位置決めは、必要なくなり補助的な役割に移行しつつある。当初は疼痛を伴うなどで安静を保てない患者は、より迅速にできると思われていたX線シミュレータで計画するなどもあったが、実際には高速のCTで計画したほうがはるかに患者にとっても楽であり治療が容易である。建築や航空機あるいは自動車教習などでの仮想シミュレータで訓練をしたほうが安全かつ容易であるのと同様であろう。さらに研修医や学生等への教育訓練の点でも非常に利点がある。

定位放射線治療

次に具体的に高精度放射線治療技術について述べる。定位放射線治療は集光照射、ピンポイント照射などともいわれる。当初は主に脳内の病変を対象として、ライナックナイフやガンマナイフとして施行されていたが、体幹部に対しても適用拡大がなされてきている。これは、比較的小さい腫瘍を対象として、非常に高い線量を病巣に投与する方法である。例えば早期肺癌の場合には現在の標準治療である手術に匹敵する制御率が達成されており、極めて低い侵襲性から高齢者、手術不能の患者にも適応可能である。

①多門照射従来法とIMRTの比較

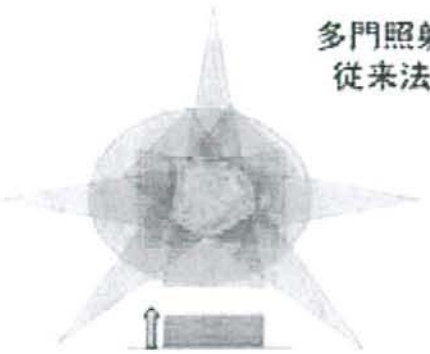

ビーム内の放射線強度は一定

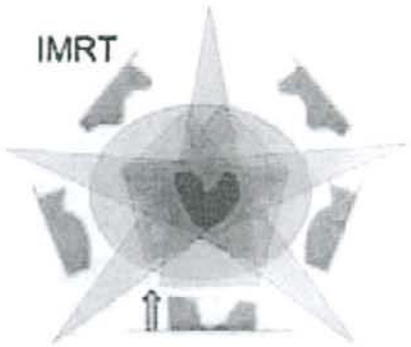

希望する線量分布より、先に強度パターンを計算
多方向投影により標的に一致した線量分布を生成

転移性脳腫瘍などに対しては1回で治療することが多いが、体幹部では数回に分割して治療する。通常の放射線治療が5、6週間を要するのに対し1週間以内で治療できる。原発性肝癌に対しても非常に高い局所制御が得られており、適応が広がっている。

強度変調放射線治療

IMRT（強度変調放射線治療）は複雑な形状の標的体積にほぼ一致させ、意図するような線量分布を得る照射法であり、コンピュータが最適なビーム配置と照射パターンを作成する（図①）。前立腺、頭頸部、中枢神経などに2008年4月より保険適応となった。最近しばしば話題になっているが、実際に試行している施設は必ずしも多くない。これは、米国ですでに大半の施設で実施されて通常の治療の一つとなっているのと比べると少なからぬ差がある。

具体的な照射方法の決定はinverse planning

という手法が用いられる。腫瘍（標的体積）をCTデータ上に3次元的に描出し、標的体積が受けるべき最低線量、危険臓器に許容される最大線量などの制限事項をパラメータとして指定する。最適化プログラムはこれらの制限をみたすように、3次元的に線量分布を計算していく。線量強度を変化させながら要求される条件を最も満たすようなパラメータの組み合わせを逐次的に繰り返して計算して最適な治療方法を求めるのである。以前はかなりの時間がかかったが、最近の最適化プログラムでは簡単な計画では数分で可能である。

②位置決めシステム搭載ライナック

周辺技術としては患者固定法や体動監視、抑止装置などが重要である。体幹部で呼吸の影響がある部分には呼吸同期照射なども研究されている（図②）。また、IMRTにおいては、照射前に照射野形状、深部線量の実測検証、治療中の精度の保証などの品質管理が欠かせない。

臨床応用

頭頸部や前立腺癌への応用が早期より行われている。とくに前立腺癌は摘出術と同程度以上の治療成績が得られており米国などでは急速に置き換わっている（図③）。併発有害事象ははるかに少なく、排尿障害や勃起障害の頻度も非常に低い。これまでの前立腺放射線外照射では

2年での直腸、膀胱からの出血などの晩期有害事象は約10％に見られるが、ＩＭＲＴでは約2％にまで激減すると報告されている。すなわちＩＭＲＴにより有害事象増加を伴わない線量増加が可能となる。上咽頭癌などの頭頸部腫瘍では手術と比べて機能障害の少ない放射線治療が

③前立腺 IMRT

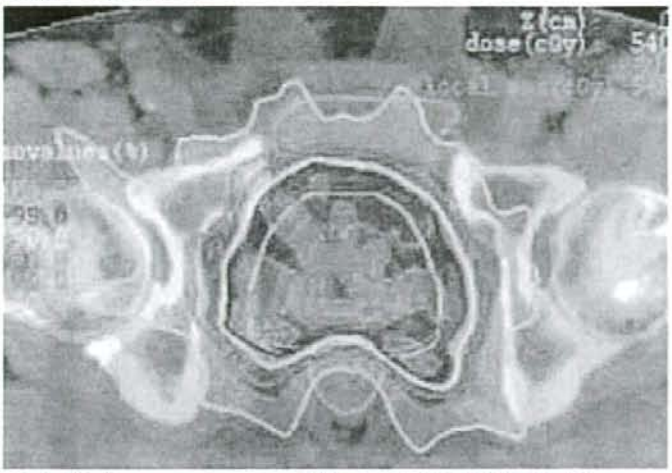

前立腺癌 T3N0M0、精嚢および皮膜浸潤疑い。
IMRT 希望され、78Gy／39回を前立腺および精嚢を target として IMRT 施行。

④肺癌の IMRT

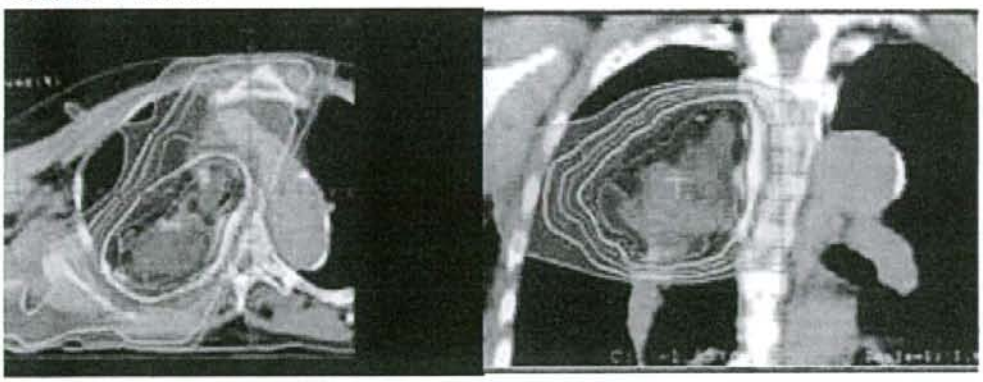

80歳代前半　男性、肺癌（扁平上皮癌）StageⅢB
上縦隔に接した右上葉の腫瘍。高齢あり総線量72Gy を正常肺の照射を避けて IMRT 治療した。

これまでも多くの部位で第一選択になっているが、ＩＭＲＴではさらに脊髄や唾液腺を避けた照射が可能であり、唾液分泌障害などを減じることができる。

脳腫瘍でも、これまでも放射線治療は重要な位置を占めているが、治療後晩期に正常組織の障害が生じることもあった。ＩＭＲＴでは脳幹が重要部分の障害を最小限にすることができる。脊索腫、神経膠腫など多くの腫瘍に適応があるが、より狭い範囲に1回または小分割で行う定位放射線治療と、比較的大きな腫瘍に分割照射で行うＩＭＲＴを使い分ける必要がある。

今後の放射線治療の展望

少し前まで一般の患者のみならず、医師の間でも放射線治療のイメージは明るいものでなく、手術のできない進行した患者に仕方がないから行う、というような印象もあったと思うが、最近では全く違ってきて、むしろ早期癌は放射線で、という時代になりつつある。また過去にはあった放射線治療後障害も現在の技術ではまず生じない。

米国では癌患者の60％以上が放射線治療を受けている。それに対してわが国では過去の放射線被爆の悪いイメージもあり、現在のところ25％程度にすぎないが、今後、米国並みに増加することは間違いない。とくにＩＭＲＴは放射線に伴う障害を激減することができるため、治療成績のみならずＱＯＬの点でも期待されている。また、今後は呼吸に同期して照射する、あるいは腫瘍の動きに追従する4次元治療が進歩するものと思われる。とくにリアルタイムに画像を見ながら治療するImage-guided radiotherapy（IGRT）は現在研究が進みつつある。

しかしこれらの高精度放射線治療は一方で非常に手間のかかる治療でもある。急増する治療に対処するには放射線腫瘍医だけでなく、医学物理士、放射線治療専門技師、癌専門看護師な

どのコメディカルの養成も重要なキーポイントであろう。とくに線量計算や精度管理に責任を持つ医学物理士が病院にはほとんどいないなど、わが国の放射線治療の構造的な問題がある。アメリカでは学位を持つ医学物理士数が約4、000人とされているが、本邦では100人程度であり、それも大部分は研究施設に勤務しており、大学病院においてすら配置されているのは稀である。医師や技師がこれまでその業務を肩代わりしていたが最近のシステムは医師ができるものではなくなっている。実際、IMRTではないが、最近いくつかの大学病院、基幹病院などで照射装置や治療計画装置に関連した極めて初歩的な放射線治療に関連した事故の報告、事故の可能性が顕在化している。高精度放射線治療は複雑なシステムである。今後もさらに発展し、高齢化社会にも適したQOLの高い治療となるであろうが、これを有効に働かせるにはやはり「人」が大事といえる。

（慶應義塾大学医学部　講師　放射線治療・核医学科）
*（慶應義塾大学医学部　教授　放射線治療・核医学科）

Detection of Perineural Tumor Invasion of the Head and Neck

Clinical Use of Thallium-201 SPECT/CT Image Fusion

Tadaki Nakahara, MD, Takayuki Suzuki, MD, Etsuo Kunieda, MD, Suketaka Momoshima, MD, Naoyuki Shigematsu, MD, and Atsushi Kubo, MD

Abstract: A patient with adenoid cystic carcinoma of the skull base was treated with radiotherapy because of perineural tumor invasion (PTI). Treatment evaluation using magnetic resonance (MR) imaging showed disease progression of PTI outside the irradiated area, whereas it was difficult to evaluate the therapeutic effect of radiotherapy because the irradiated lesions still had contrast enhancement. Thallium-201 SPECT/CT image fusion was performed to evaluate tumor extent and viability after therapy. During the follow-up period, disease progression was noted in the areas of abnormal uptake on the thallium-201 SPECT/CT fusion images, but the lesions with no uptake remained unchanged on follow-up MR imaging. Thallium-201 SPECT/CT image fusion can be used for precise localization of viable PTI in head and neck cancer patients who had been previously treated.

Received for publication May 22, 2007; revision accepted March 24, 2008.
From the Department of Radiology, Keio University School of Medicine, Tokyo, Japan.
Reprints: Tadaki Nakahara, MD, Department of Radiology, Keio University School of Medicine, 35 Shinanomachi, Shinjuku-ku, Tokyo, 160-8582, Japan. E-mail: n-tadaki0909@k6.dion.ne.jp or dnakanaka@yahoo.co.jp.

ISSN: 0363-9762/08/3308-0567

Key Words: SPECT/CT, perineural tumor invasion, thallium-201, radiotherapy, adenoid cystic carcinoma

(*Clin Nucl Med* 2008;33: 567–570)

REFERENCES

1. Nakahara T, Shigematsu N, Fujii M, et al. Value of CT thallium-201 SPECT fusion imaging over SPECT alone for detection and localization of nasopharyngeal and maxillary cancers. *AJR Am J Roentgenol.* 2006; 187:825–829.
2. Bhatnagar AK, Heron DE, Schaitkin B. Perineural invasion of squamous cell carcinoma of the lip with occult involvement of the infra-orbital nerve detected by PET-CT and treated with MRI-based IMRT: a case report. *Technol Cancer Res Treat.* 2005;4:251–253.
3. Conrad GR, Sinha P, Holzhauer M. Perineural spread of skin carcinoma to the base of the skull: detection with FDG PET and CT fusion. *Clin Nucl Med.* 2004;29:717–719.
4. Fosko SW, Hu W, Cook TF, et al. Positron emission tomography for basal cell carcinoma of the head and neck. *Arch Dermatol.* 2003;139:1141–1146.
5. Nakahara T, Fujii H, Hashimoto J, et al. Thallium-201 single-photon emission computed tomography in the detection of retroperitoneal schwannoma. *Br J Radiol.* 2004;77:57–59.
6. Gandhi D, Gujar S, Mukherji SK. Magnetic resonance imaging of perineural spread of head and neck malignancies. *Top Magn Reson Imaging.* 2004;15:79–85.
7. Yousem DM, Gad K, Tufano RP. Resectability issues with head and neck cancer. *AJNR Am J Neuroradiol.* 2006;27:2024–2036.
8. O'Tuama LA, Poussaint TY. Thallium-201 single-photon emission CT in recurrent squamous cell carcinoma of the head and neck. *AJNR Am J Neuroradiol.* 2002;23:174–175.